JOURNAL OF CHEMOMETRICS
J. Chemometrics 2006; **20**: 311–320
Published online in Wiley InterScience
(www.interscience.wiley.com) DOI: 10.1002/cem.1029

Crispness assessment of roasted almonds by an integrated approach to texture description: texture, acoustics, sensory and structure

P. Varela[1], J. Chen[2], S. Fiszman[1] and M. J. W. Povey[2]*

[1]Instituto de Agroquímica y Tecnología de Alimentos (CSIC) Apartado de Correos 73, 46100 Burjassot, Valencia Spain
[2]Procter Department of Food Science, University of Leeds, Leeds LS2 9JT, UK

Received 16 May 2006; Revised 15 December 2006; Accepted 22 December 2006

This study combines passive acoustic and mechanical measures of sensory crispness. We show that the acoustic signal is dominated by 'bursts' of sound associated with crack failure events in the product which also release measurable amounts of elastic energy. One-way analysis of variance (ANOVA) and principal component analysis (PCA) were performed on the sensory, acoustical, mechanical and compositional parameters. We show that this chemometric approach is a powerful method for the objective analysis of large, complex data sets in the context of human sensory studies and the objective measure of a sensory parameter; in this case crispness. We demonstrate that sensory crispness in almonds is an amalgam of acoustic and mechanical effects occurring during chewing. We show that our method is capable of predicting the crispness of roasted almonds. Copyright © 2007 John Wiley & Sons, Ltd.

KEYWORDS: crispness; texture; sound; sensory; microstructure; PCA; almonds

1. INTRODUCTION

The distinction between the two multidimensional sensory attributes crispness and crunchiness is not yet fully understood; but we know that they are directly related to the mechanical and fracture properties of solid food materials, to their macro and microstructure and to the way they are eaten [1,2]. Different approaches have been used for crispness evaluation, sensory tests, instrumental texture and sound analyses, as well as microstructural observation since Szczesniak [3,4] highlighted the importance of food crispness for consumers, and Vickers, Bourne and Drake [5,6] related the perception of this attribute to the auditory sensations. Studies on crispness/crunchiness assessment can be found in the literature over the last 50 years [7]. Recently, some interesting reviews have been published on the subject [8–10]. These summarise the various methods used and pinpoint two principal approaches taken in the study of crispy/crunchy textures using acoustic techniques: the measurement of the perception of air-conducted sounds to establish its contribution to the sensation of crispness, and the recording of the sounds while performing a mechanical test. The advantage of this approach is that all aspects of fracture are well controlled. In the first case, these authors played pre-recorded bite and chew sounds to subjects to assess crispness, or asked them to chew or bite and to evaluate the sound, or a combination of both. The results obtained permitted the development of definitions of crispy, crunchy and crackly and the suggestion of the possible differences between the terms, which are still controversial. They also showed that subjects could still assess crispness when auditory blocking was applied during consumption of a food, suggesting that crispness was to some extent, a vibro-tactile sensation. The combination of acoustic recording with mechanical tests results in a more controlled and objective way of analysing sound emission and allows the extraction of a number of parameters for correlating to sensory measurements. To study the sounds generated at fracture, previous studies either analysed the amplitude-time plot of the acoustic signal, or the amplitude-frequency using Fast Fourier Transform, extracting parameters like amplitude, mean height of peaks, number of sound bursts, mean sound pressure level (SPL), etc. The three cited reviews agree on the fact that although some progress has been made in the field of texture assessment of crispy/crunchy products, much remains unknown, and in future the relation between acoustic, physical, sensory and structural properties of the food materials needed to be integrated.

In 2005 Chen *et al*. [2] showed that the use of an Acoustic Envelope Detector (AED) attached to a TAXT Plus (SMS)

*Correspondence to: M. J. W. Povey, Procter Department of food Science, University of Leeds, Leeds LS2 9JT, UK.
E-mail: m.j.w.povey@food.leeds.ac.uk

Texture Analyser was effective in detecting the acoustic emission of biscuits at rupture. They found an excellent correspondence between the recorded sound analysed as the number and maximum amplitude of sound bursts, the second derivative of the force curve in a bending test and the sensory assessment of crispness. Recently Courcoux *et al.* [11] used acoustic emission only as an objective measure of crispness in cereal flakes, demonstrating the limitations of previous work with regard to data analysis technique. For example, Tesch, Normand & Peleg [12] were not able to establish a relationship between the mechanical and acoustic signature obtained for cellular cereal foods by compression, attributing it to the different sampling rates of the measurements or to the difference between samples.

Almonds have a crispy/crunchy nature, sometimes enhanced by roasting. Spain is the world's second almond producer [13]. Its cultivation has risen in the last years, particularly in the south-eastern region, where the principal variety is *Marcona*, mostly consumed as a roasted or fried snack. Convection oven, the most common roasting system, causes changes in appearance, texture and flavour, due to dehydration, browning, lipid oxidation and diverse structural changes [14,15]. The degradation of the structure during roasting could cause changes in textural properties like crispness, hardness, grittiness, porosity, fracturability, etc., which in turn would affect the characteristics of the noise emitted on eating.

Almonds were chosen as study material because crispness/crunchiness is a key factor in the acceptability of roasted almonds. Little research has been done on almond texture in spite of the fact that they are very important to the Spanish market. In addition, the considerable differences between almonds and biscuits provided a useful comparison with our previous work [2]. The aims of this work were to assess the crispness of *Marcona* almonds with different degrees of roasting by means of an integrated approach: the simultaneous measurement of force/displacement on compression of the emitted sound, and their relation to the structure, microstructure and sensory assessment. In order to meet the challenge of the complexities offered by almonds as a natural and heterogeneous material, we applied chemometric methods of analysing acoustic and mechanical data, which are of general applicability to complex heterogeneous materials that fail by cracking.

2. MATERIALS AND METHODS

2.1. Testing materials

Raw, peeled *Marcona* almonds (*Prunus amygdalus* L.), purchased in a local supermarket were divided into five batches; four were roasted in a convection oven, at 200° C, for 1.5, 3.0, 4.5 and 6.0 min. When they reached ambient temperature, they were placed in airtight containers (rigid polypropylene) and placed in a refrigerated chamber until analysis.

Additionally, the almonds were selected according to their size and shape, to ensure the minimum variation within a batch, with dimensions: length 22 ± 1 mm, width 14 ± 1 mm, height 7 ± 1 mm, and weight 1.2 ± 0.1 g. This was to aid consistency in the mechanical testing.

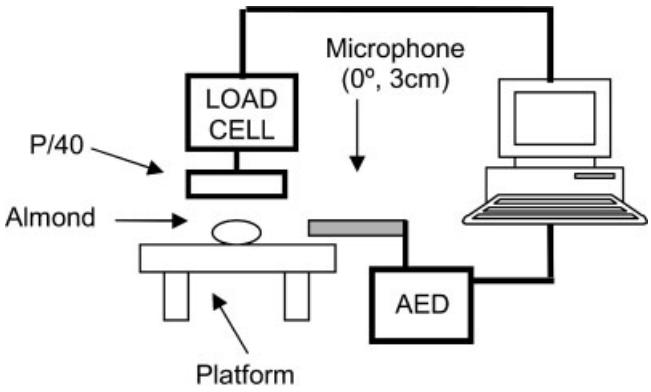

Figure 1. Diagram of the instrumental setup for the texture/acoustic measurement.

2.2. Instrumental analyses: texture and acoustics

A TA-XT plus Texture Analyser (Stable Micro Systems, Godalming, UK) was used for force/displacement measurement with a 30 kg load cell, together with a P/40 cylinder (40-mm diameter) used for the compression tests. The test settings were: test speed 1 mm/s, target mode: strain, strain 50%, trigger 10 g. An AED described in detail elsewhere [2] was used for sound recording together with the corresponding software (Texture Exponent 32). The gain of the AED was set at one. A Bruel and Kjaer free-field microphone (diameter 8-mm), calibrated using an Acoustic Calibrator Type 4231 (94 and 114 dB SPL-1000 Hz) was positioned at 3 cm distance and with an angle of 0° to the sample (Figure 1). This angle minimised the distortion that the probe created in the sound field. A high pass filter of 1 kHz removed extraneous ambient acoustic and mechanical noise. A low pass filter set the upper calibrated and measured frequency at 16 kHz. The AED operates by integrating all the frequencies within the band pass range generating a voltage proportional to the SPL. The integration time was set at 0.25 ms. The data acquisition rate was 500 points per second for both force and acoustic signals. All tests were performed in a laboratory with no special soundproof facilities, with a relative humidity of around $25 \pm 1\%$, and a temperature of 22 ± 2° C. Each test was performed on six almonds from each batch (the raw one and the four different roasting times—six replications on each sample). Force versus displacement and SPL versus displacement were plotted, the parameters extracted from the curves and their units are displayed in Table I.

2.3. Sensory analysis

A panel of eight assessors of the Procter Department of Food Science of the University of Leeds, experienced in crispness assessment was used. The assessors were blindfolded so that no visual interference was involved in the perception of crispness, and they were fed with the samples to avoid tactile interference. They received one almond of each different roasting time and one raw, following a balanced complete block experimental design. For each sample, they had to quantify the attribute *crispness* by introducing the whole almond into their mouth and chewing the sample. They used a 9-box scale labelled on the left with 'nil' and on the right

DOI: 10.1002/cem

Table I. Definition of the instrumental parameters extracted from the force/displacement and sound pressure level (SPL) curves

Parameter	Definition	Units
Area	Area of the force curve (related to the work of compression)	N.sec
$Slope_{Fmax}$	Slope of the linear part of the force curve to the first force breakdown	N/sec
Number of force peaks	Number of peaks of force, using a threshold value of 0.05 N	—
Average gradient	Average gradient of all positive slopes (through to peak)	N/sec
Fit distance	Sections are calculated as a line between the mid points of the force peaks and troughs. The length of each section is calculated using sqr($y^2 + x^2$) where y is the change in force in newtons and x is the change distance millimetres. The length of each section is then added together to form the Fit Distance	—
Average drop off	The average drop in data between consecutive peaks and troughs	N
Linear distance	The length of an imaginary line joining all points in the selected region. A highly jagged line, with lots of fluctuations in force due to many fracture events, has a length much longer than a smooth line resulting from the testing of a similar 'soft' product	(N.sec)
Force at failure	Force value of the first force breakdown, using a threshold value of 0.05 N	N
Distance at failure	Distance of the probe in the first force breakdown	M
Number of sound peaks	Number of peaks of the sound plot, using a threshold value of 2.5 dB	—
Max SPL	Maximum peak intensity of the SPL	dB

with 'high' to assess the *crispness* level. At the same time, a microphone was positioned in front of the assessors within a distance of 3 ± 1 cm away from the mouth and acoustic signals were recorded. The microphone used was the same as in the mechanical tests.

2.4. Macrostructural and microstructural study

Macro-structural observation photographs were performed with an Intel® Play™ QX3™ Computer Microscope (Intel®, San Diego) using the $\times 10$ magnification setting.

Microstructural analysis was performed by Environmental Scanning Electron Microscopy (ESEM) on the raw and 6 min-roasted samples. A Philips XL30 ESEM (Oxford Instruments, Oxford) was used. The samples were compressed with the texture analyser as in the texture/sound tests and the fractured surfaces obtained were observed. Experimental conditions were 30 kV accelerating voltage, a temperature of 4°C, and a pressure of less than 5.2 torr.

2.5. Compositional analyses: moisture and total fat contents

Moisture was determined by vacuum drying at 95° to constant weight, AOAC method 925.40. Total fat content was determined by direct extraction with ether in a Soxhlet extractor, AOAC method 948.22 [16]. Four replications were performed for each determination.

2.6. Statistical analyses and data acquisition constraints

One-way analysis of variance (ANOVA) was performed on the sensory, instrumental and compositional parameters; also principal component analysis (PCA) was done to illustrate the correlation among them. Both were performed with the use of the SPSS 12 package. The rotation method used was Varimax with Kaiser normalization, and loadings were taken into account if their absolute value was higher than 0.6 (Table IV). The derivative analysis was performed with Origin Lab 7.

The data analysis method developed in Chen *et al.* [2] was followed but with the following important differences and caveats. The second derivative of the force curves (using 11-point Savitzky-Golay smoothing) was used to study the correlation with the sound plots.

3. RESULTS AND DISCUSSION

3.1. Analysis of the force/displacement and acoustic plots

The test speed 1 mm/s was selected based on previous tests, reaching a compromise of having reproducible and discriminative force curves, where the fracture events are controlled, and also where sound peaks could be distinguished. Figure 2 shows two examples (raw and 6-min roasted samples) of the force versus displacement of the probe and the SPL versus displacement plots. In both cases the curves are displayed together as it appeared in the controller computer screen when performing the test, the signals were synchronized, allowing the comparison in real time of the force and sound data.

The force curves presented two regions, the first part, where the force increases with the displacement, and which is a function of the rigidity, shape and size of the material, the sample is subjected to deformation but no major structural breakdown occurs, so the sample is acoustically 'very quiet' [1,2]. Roasting causes a decrease in toughness in the material: the force and strain of the material failure decreased, the first breakdown is recorded at about 200 N in the raw sample, while it occurred at about 70 N in the 6-min roasted almond, and at a lower distance of the probe [2].

The second part of the curve is considered to begin at the point where the first structural breakdown occurs and the sample starts to break. Then, depending on the brittleness of the material, a sudden decrease of the force values occurs, the fracture propagates up to an inhibition of the fracture due to the presence of some crack stopper, and then it starts again as the almond is further deformed. At the end of the test, the force is high, as the sample is being further compressed and

DOI: 10.1002/cem

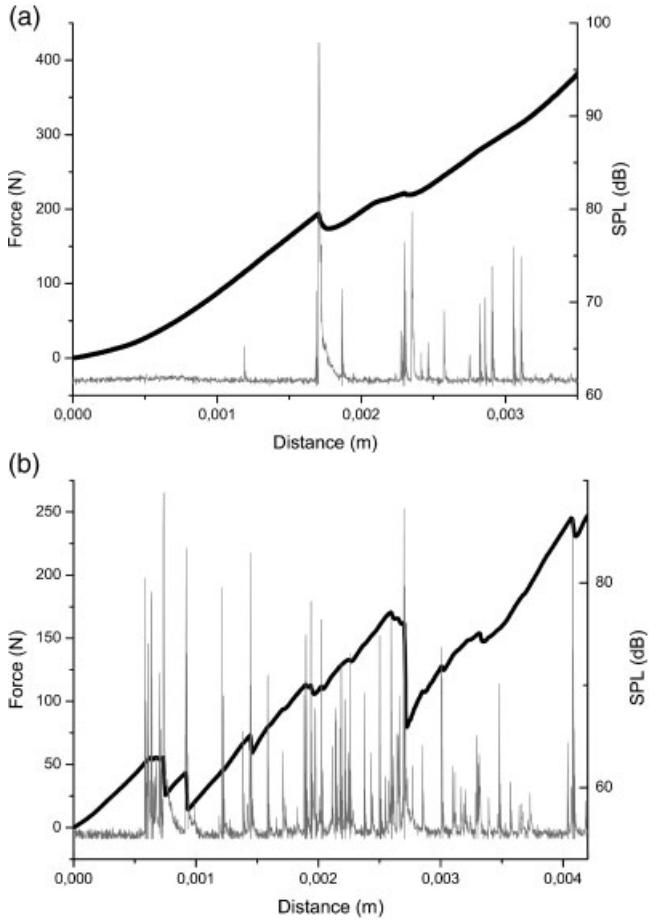

Figure 2. Force (black line) and sound pressure level (SPL; grey line) versus distance in compression: (a) raw almond, (b) 6-min roasted.

the density increased [1,17]. Comparing both force curves, it is clear that the 6-min roasted almond is more brittle (Figure 2(b)): the plot is very jagged, there are many sudden drops in force, reflecting fractures of rapid propagation, and many acoustic events were recorded within a short period. In the raw almond (Figure 2(a)), only two small drops in force can be detected, and a much smaller number of acoustic events were detected.

In both examples showed in Figure 2, for each major force drop a group of acoustic events seemed to happen and many sound events did not appear to be directly related to drops in force. However, they do not have to be correlated one-to-one, as the sound emission is the result of a sudden release of energy, while the force curve is a reflection of the energy applied to, or released from the sample.

During the deformation of a material, stress will build up inside it, and the crack will start at the weakest point as the stress exceeds the yield point, if the speed of the crack propagation is high, the energy dissipated from the structural failure will spread out as audible shock waves [2,17]. In general, when a crisp material is broken, it is hypothesised that each fracture event corresponds to an acoustic event [2,18,19]. A feature of our analysis technique is that the mechanical data are analysed chemometrically together with the acoustic and sensory data. To do this we first derive the second derivative of the force-displacement curve. We have found that if this is not done, correlations between acoustic and mechanical data are much poorer [2]. This necessary derivatisation means that the maximum measurable rate of crack events is 45 crack events per second. This is an unavoidable price to be paid if the mechanical and acoustic data are to be correctly analysed. Ideally, we would like to increase the sampling rate of the mechanical system to ten times above that of the maximum frequency detectable in the human mouth. The second significant difference to our previous work [2] is the use of the logarithm of the modulus of the negative values of the second derivative only, rejecting the positive values from the analysis. There are two reasons for doing this. Firstly, it is well known that human sensory experience generally responds to stimulus logarithmically. This is why acoustic pressure is expressed in decibels rather than as pure acoustic pressure, since the audible intensity ranges from 10^{-12} to 10 Watts/m^2[20]. It is reasonable to assume that this is also the case with forces in the mouth, which our mechanical tests are mimicking. Secondly, the second derivative of the force curve is a measure of the rate of change of elastic energy in the sample as it is stressed. However, the second derivative reflects both the storage and the release of energy and it is clear from the mechanisms involved in the creation of crispy sensations that the crack events that generate these sensations will be correlated in time with energy release, not energy storage.

Figure 3(a) displays the second derivative of the force curve and the SPL plot for the 6-min roasted sample. The correspondence between the plots is still poor; however, it seems clearer just for the big cracks already visible in the force curve. Many sound peaks cannot be explained by applying the second derivative analysis. In Figure 3(b) we show the correspondence of the SPL plot to the mechanical data, using the negative part of the second derivative of the force curve only, plotted on a logarithmic scale. In contrast to Figure 3(a), we see that now most of the sound peaks have a corresponding peak in the second derivative. Moreover, not only does the occurrence of the peaks correspond but also does the shape of the curves, as can be appreciated in the enlarged zone presented in Figure 3(c). This is a surprising finding, as it suggests that mechanical and acoustic data are correlated and display related information if adequately analysed. The number and intensity of acoustic events registered by the detector would therefore depend on the development of the fracture, in particular on the rate of change of energy release of the sample being fractured. Vincent [1,18] stated that the disadvantage of the acoustic approach was that the signal could not be translated into materials science terms or the events could not be associated with specific fracture energies. On the contrary, Luyten *et al.* [17,19] hypothesised that energy dissipative processes were crucial for understanding the crispy/crunchy nature of solid foods, but hitherto they have been neglected in most research studies. Our integrative data analysis approach is a step in that direction, relating sound emission with energy release.

From the plot obtained (Figure 3(b)) the peaks were counted, using a threshold of 10^9, determined by the derivation of the first part of the force curve (second derivative), before the first breakdown, where there was no acoustic event detected.

DOI: 10.1002/cem

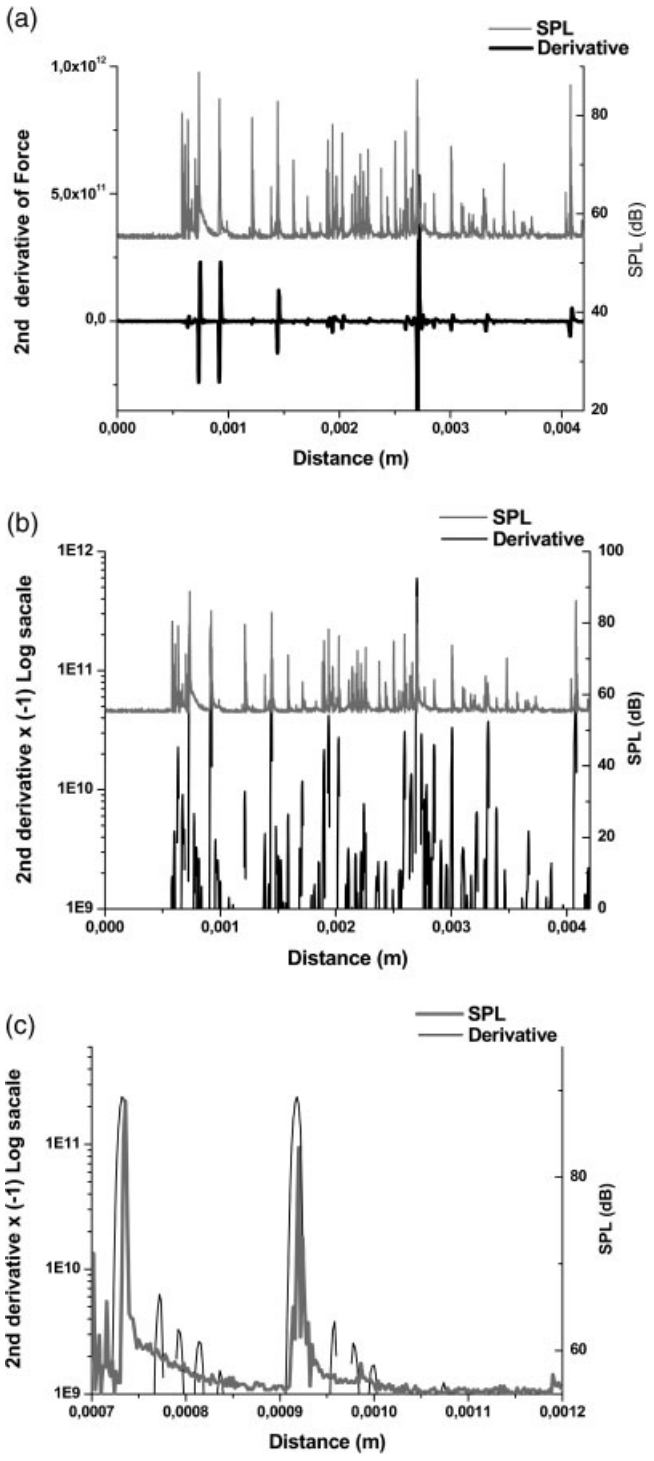

Figure 3. Correspondence of force (black lines) and SPL plots (grey lines), example for the 6-min roasted sample, (a) using the second derivative of the force curve, (b) using the negative values of the second derivative of the force curve, (c) Enlarged section of Figure 3(b), correspondence of the shapes of the force and SPL plots, using the negative values of the second derivative.

3.2. Analysis of the mechanical and acoustic parameters

From the parameters calculated from the curves (Table II) it can be appreciated that the value of the first force breakdown (force at failure) was significantly lowered with roasting and

Table II. Mean values of the instrumental parameters extracted from the force/distance, force derivative/distance and the SPL/distance plots

Sample	Area (N.sec)	$Slope_{Fmax}$ (N/sec)	Number of force peaks	Average gradient (N/sec)	Fit distance	Average drop off (N)	Linear distance (N.sec)	Force at failure (N)	Distance at failure (m)	Number of peaks of the derivative	Number of sound peaks	Max SPL (dB)
Raw	609.3^{a}	51.2^{a}	3^{a}	125.1^{a}	75.0^{a}	$55.9^{b,c}$	790.6^{a}	$198.1^{b,c}$	1.83E-03^{b}	34^{a}	20^{a}	85.6^{a}
1.5 min	789.5^{b}	83.6^{b}	3^{a}	131.8^{a}	53.4^{a}	789^{c}	996.4^{c}	239.7^{c}	1.83E-03^{b}	$43^{a,b}$	18^{a}	$89.5^{a,b}$
3.0 min	863.2^{b}	78.7^{b}	4^{a}	111.1^{a}	31.6^{a}	7.6^{a}	$906.1^{b,c}$	157.7^{b}	1.33E-03^{a,b}	$51^{b,c}$	36^{a}	$93.4^{a,b}$
4.5 min	817.7^{b}	77.7^{b}	9^{b}	115.5^{a}	46.3^{a}	$9.8^{a,b}$	$978.8^{b,c}$	169.2^{b}	1.50E-03^{a,b}	60^{c}	107^{b}	105.2^{b}
6.0 min	605.3^{a}	83.2^{b}	18^{c}	117.9^{a}	55.3^{a}	$11.1^{a,b}$	888.0^{b}	71.8^{a}	1.00E-03^{a}	77^{d}	141^{c}	102.3^{b}

Averages of six replicates. Identical letters indicate that there is no significant difference at $p > 0.05$.

DOI: 10.1002/cem

it occurred earlier, showing enhanced brittleness because of the thermal processing. However, the value of the slope of the first part of the force curve, which can be related to the rigidity of the samples, was lower in the raw sample, but remained unchanged with the different roasting times. The work required to compress the samples (area under the curve) increased initially with the roasting time but started to decrease from 4.5-min roasting. This reflects the change of the mechanical nature of the almonds, from tough (strong and slightly deformable) to brittle (hard and weak). The 'average gradient' and 'fit distance' did not present significant differences between the samples. The 'number of force peaks' and the parameters 'average drop off' and 'linear distance' also showed the rise of brittleness and crispness with roasting. The values reflected the fact that the roasted samples undergo a larger amount of fracture events, related to a more crispy/crunchy texture [1]. The number of peaks of the sound plot and the number of peaks of the second derivative plot had similar trends, increasing with roasting, and in agreement with the mechanical observations, because the number of peaks of the second derivative was even more discriminating between samples. The maximum of the SPL is significantly higher for the roasted almonds than the raw.

3.3. Structure, microstructure and composition, relation to the fracture behaviour

We have stated that the sound emission in compression depends on the mechanics of the fracture, which in turn depends on the parameters of the compression and on the shape, size, structure and microstructure of the sample. The irregular peaks observed in the force curves of the roasted samples, characteristic of a crispy/crunchy product, reflected multiple fracture events, and could be a result of a non-homogeneous morphology; microstructural elements such as water or oil phase distribution causing the anisotropy of the structure. However, the particular importance of these elements in the perception of crispiness/crunchiness is still unknown [1,17,21]. Thus, study of food structure in relation to fracture mechanics is of great interest. Figure 4 shows photographs of two almond samples fractured after the compression test. A great difference in the breakage pattern can be seen between the two samples. The raw sample subjected to compression is deformed in the first step of the compression test, being fractured as a result of the tensile forces developed and concentrated in the two ends of the short axis—because of the shape and dimensions of the sample—and causing the 'opening' of the sample. This behaviour was clearly reflected in the force plot, which has a long elastic first part, and two noticeable fracture events, and in the not very jagged acoustic plot. In the case of the 6-min roasted almond, the material was drastically changed, it became much less resistant to the compression, the elastic deformation zone was small, and the material collapsed because of the compression forces on the surface, fracturing in many directions. The rapid breakdown and the many fractures were reflected in the force and sound plots.

Fracture in food materials starts in inhomogeneities and will travel quickly until a crack stopper, such as an air pocket, empty space or starch granule inhibits it. In these cases, heterogeneity is as important to crispness as brittleness [1,17]. The microstructure was observed by ESEM in order to study what caused the change in the fracture behaviour of the almonds because of roasting. ESEM is a technique that allows samples to be observed in an electron microscope with minimal preparation (no drying, coating or staining) other than producing a sample of the correct size. Changes in biological tissues can be studied close to their native state and at relatively high resolution [22,23].

Figures 5(a) and b show the ESEM photographs of the fractured surfaces of the two extreme almond samples (raw and 6-min roasting). The raw sample presented a cleaner fracture, more even, and some of the cells seemed to have been taken away to the other side of the cut. These facts support the idea previously stated, the sample failed as a result of the resultant tensile forces because of the shape of the food item as much as the failure of the material itself. The roasted almond showed an uneven fractured surface, very heterogeneous, with the presence of cell material outside the cells. Pascual-Albero *et al.* [14] observed this phenomenon and attributed it to protein agglomerations or coalesced lipids that exited the cells with the heating process. In the present work, based only on ESEM data, we cannot tell the difference between different kinds of cell material, but some extra cellular material appeared, increasing heterogeneity. Whereas the total lipid content remained constant at all roasting times (Table III), if this extra cellular material was

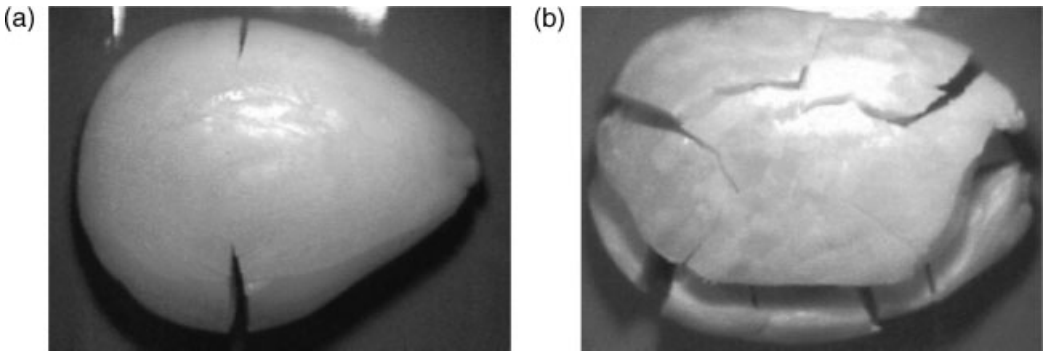

Figure 4. Photographs of the almond samples fractured after compressing in the texture analyser, examples of (a) raw and (b) 6-min roasted.

DOI: 10.1002/cem

Table III. Mean values of the moisture and fat contents

	Raw	1.5 min	3.0 min	4.5 min	6.0 min
Moisture (%)	6.1[a]	4.8[b]	2.7[c]	1.1[d]	0.8[e]
Fat (% on dry basis)	57.9[a]	57.9[a]	58.6[a]	59.8[a]	57.2[a]

Identical letters indicate that there is no significant difference at $p > 0.05$.

lipid, it would have reordered inside the almond and was not removed in the roasting process as it reached the outer surface (via the oven rack, containers, manipulations).

The outer surfaces of the raw and 6-min roasted almonds were observed before fracturing (Figure 5(c,d). The raw sample presented a very homogeneous surface composed of long cells of uniform size, ordered in a parallel pattern. This cell shape and organisation is typical of the outer epidermis beneath the testa (as the samples are peeled); and it has been previously observed by SEM in raw *Marcona* almonds [14] and the same organisation but with more irregularly outlined cells in *Nonpareil* raw almonds [24]. The roasting process also had its effects on the surface: the escape of water vapour damaged the epidermis, and some failures and perforations were noticed. Pascual-Albero *et al.* [14] reported the same kind of damage in their work on almonds roasted at 150° for 45 min with the use of SEM. The utilisation of ESEM in this work permitted a more detailed observation of the outer epidermis in non-manipulated conditions of the tissue. ESEM ensured that the changes were caused by the roasting process and not by the sample preparation. Our observations showed that the cells lost their shape and increased their volume, the parallel pattern of the cells disrupted, with some parts of the structure particularly damaged; presumably permitting the escape of cytoplasmatic material from the cells of both epidermis and parenchyma.

As the samples were heated, the low amount of water contained in the cells evaporates and tends to exit them and reach the exterior of the almond [14], this is supported by the compositional data (Table III). The water content of the samples significantly decreased with all roasting times. In addition, the total volume of pores filled with air is increased by roasting [15]. These two fluids exit the almond cells, exert a pressure and cause failures in the food material. Then, adding up all the effects: the rise in heterogeneity, the damage to the individual cell walls, and the creation of fractures because of the elimination of water, explains enhanced brittleness and crispness, as well as the fracture behaviour. The material became much less resistant to the compression, had a small elastic deformation, and collapsed as a result of the compression forces on the surface, fracturing rapidly and in many directions.

3.4. Sensory analysis

Sound was recorded for the first 15 s while the assessors chewed the almonds. Figure 6 shows, as an example, two sound plots (raw and 6-min roasted sample) for one of the assessors. The increased jaggedness in the roasted almond's plot is evident. The SPL decreased with the mastication in both cases, the sound emission almost disappears at the end of the 15 s of chewing the raw sample.

In Figure 7, the correspondence of the mechanical, acoustic and sensory data is shown by plotting the number of peaks of the sound recorded both in the sensory test and in the compression test, and the number of peaks of the negative

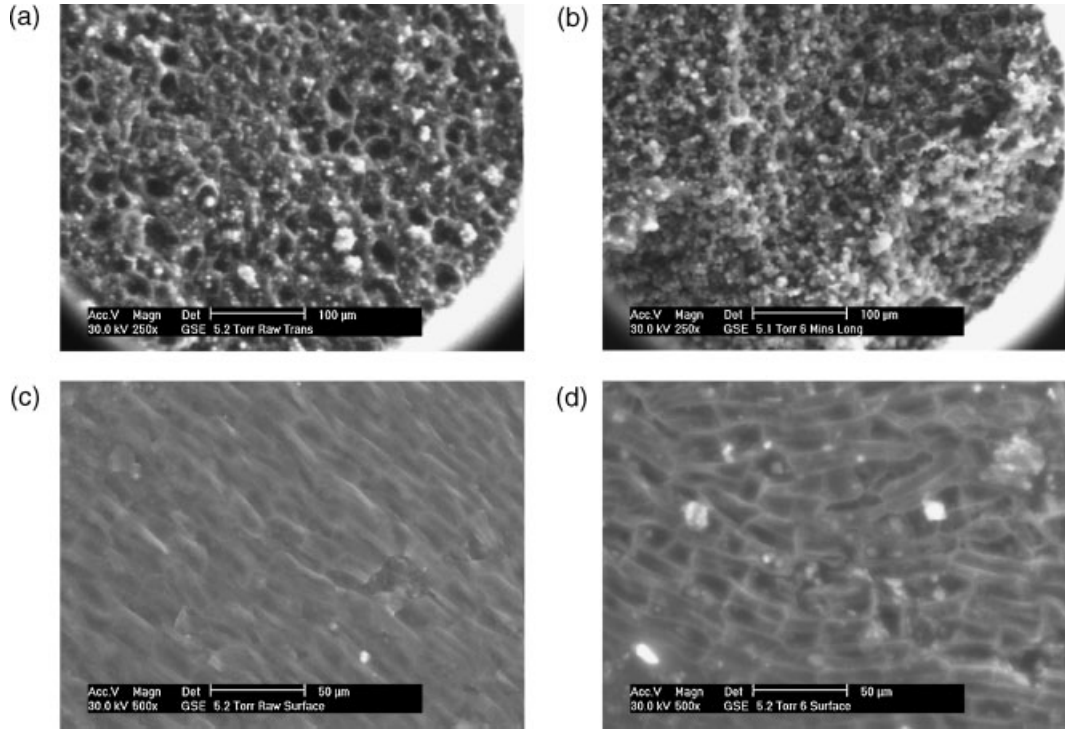

Figure 5. Microstructure (ESEM) of the almond samples: fractured surfaces (a) raw and (b) 6-min roasted; external surface (c) raw and (d) 6-min roasted.

DOI: 10.1002/cem

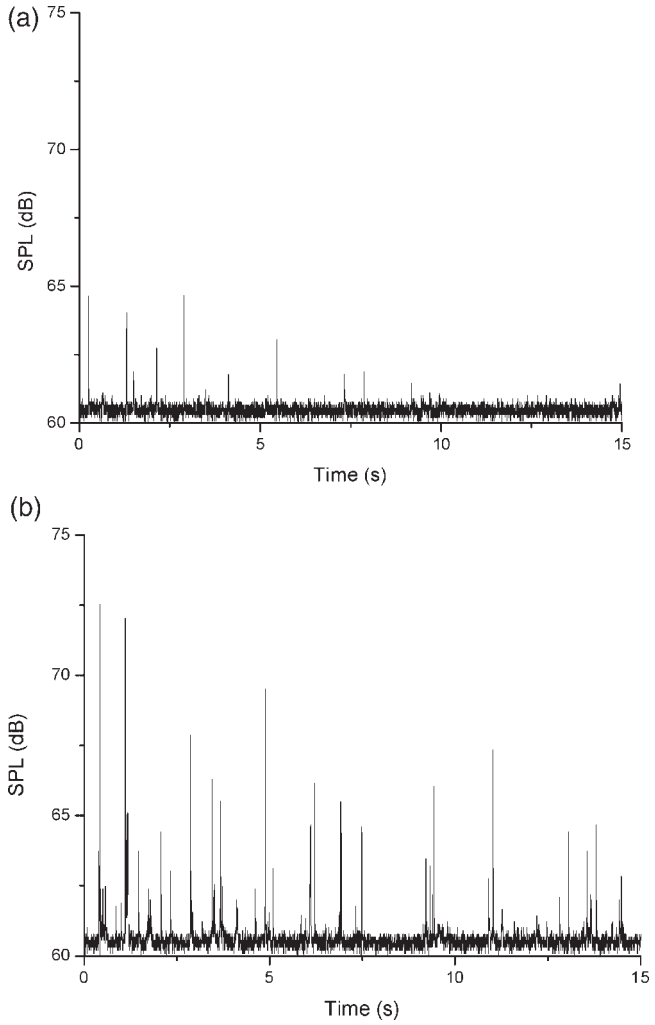

Figure 6. Sound pressure level. Example of a recording from one of the assessors while chewing the samples: (a) raw sample and (b) 6-min roasted sample.

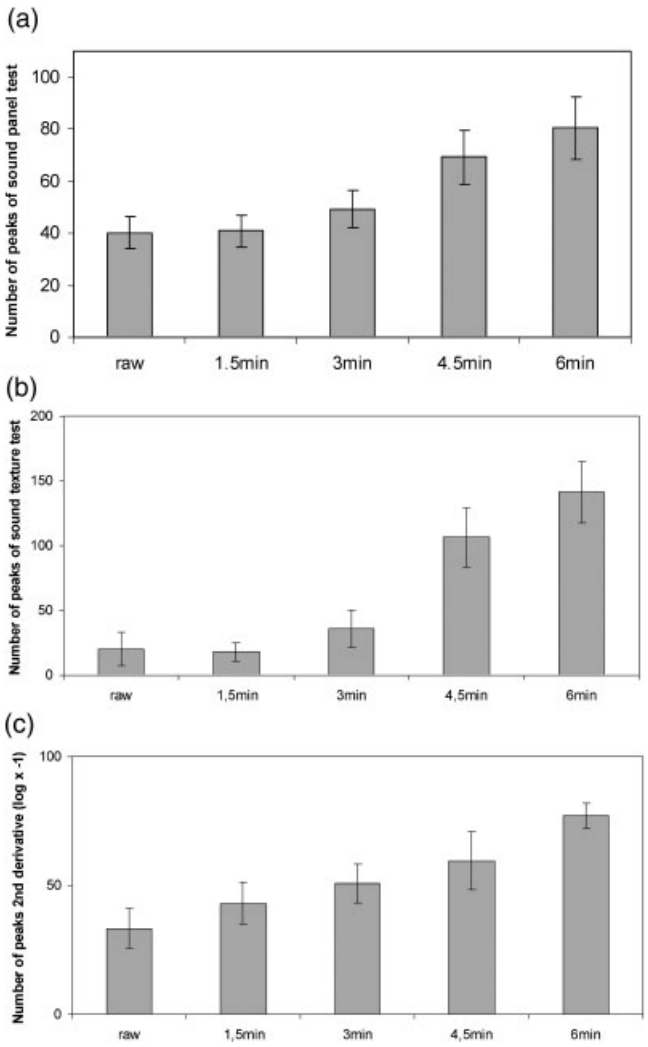

Figure 7. Effect of roasting time on the number of acoustic signal peaks: (a) sensory texture evaluation, (b) instrumental texture evaluation, (c) second derivative of force curve.

part of the second derivative. The occurrence of the three parameters was very similar.

3.5. Correlations: principal component analysis

Five components were extracted that together explain 81.9% of the variance (Table IV). Figure 8 displays the three-dimensional plot of the samples in the space determined by the first three principal components (PC), which together explain 65.7% of the variance. The analysis was able to separate the samples into groups according to the parameters that account for the variance of each of the axis. The first PC explains 39.1% of the variance, and it is composed of a combination of mechanical, acoustical and sensory parameters. The first PC showed a positive correlation to the panel sensory crispness, the number of peaks of sound, the number of peaks of the derivative, and the number of peaks of force, it has a negative correlation to the force at failure and the distance at failure. Thus, the factors already explained by the study of the force, acoustics and derivative plots are confirmed, and as discussed before, in agreement with the explanations found in the observation of structure, microstructure and fracture behaviour. In our previous work

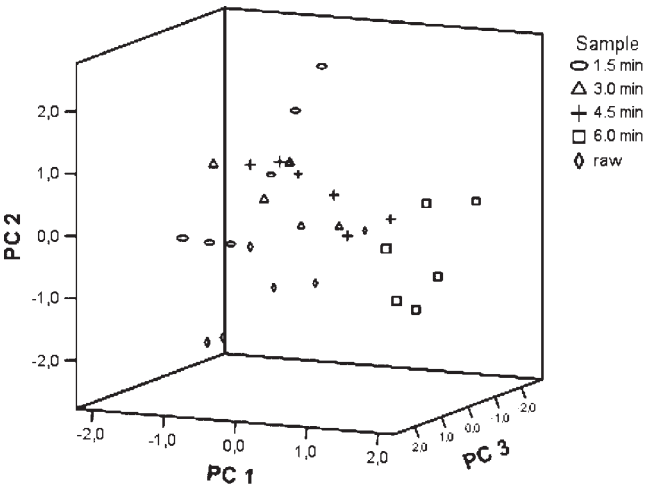

Figure 8. PCA. 3D-loading plot of the samples in the first three principal components, together they explain 65.7% of the variance.

DOI: 10.1002/cem

Table IV. Principal component analysis

	PC1 (39.1%)	PC2 (16.8%)	PC3 (9.7%)	PC4 (8.6%)	PC5 (7.7%)
Área	−0.298	**0.788**	0.360	−0.144	−0.001
$Slope_{Fmax}$	0.358	**0.666**	−0.139	−0.219	−0.042
Number of force peaks	**0.935**	−0.112	0.164	0.067	−0.013
Average gradient	−0.178	0.102	−0.002	−0.037	**0.922**
Fit distance	0.065	−0.067	−0.226	**0.854**	0.066
Average drop off	−0.446	−0.074	0.126	**0.656**	−0.349
Linear distance	−0.072	**0.823**	0.241	0.214	0.332
Force at failure	**−0.868**	0.174	0.028	0.303	0.230
Distance at failure	**−0.736**	−0.019	0.065	0.430	0.161
Number of peaks of the derivative	**0.859**	0.261	0.289	0.146	0.068
Number of sound peaks	**0.905**	0.036	0.306	−0.075	0.043
Max SPL	0.534	0.559	−0.214	−0.056	−0.077
Panel sensory crispness	**0.780**	0.248	0.256	−0.046	−0.194
Panel number of sound peaks	0.448	−0.098	**0.727**	−0.074	0.230
Panel Max SPL	0.210	0.273	**0.777**	−0.114	−0.164

Rotated component matrix. Extraction method: Principal component analysis. Rotation method: Varimax with Kaiser normalization. Rotation converged in 16 iterations. Correlations were taken into account if their absolute values were >0.6 (numbers in bold print).

on biscuits [2], the first principal component was dominated by acoustic measures whilst the second PC was dominated by mechanical ones. In contrast, in almonds, the first PC contains both acoustic and mechanical measures. The second PC (16.8%) includes three force parameters (area, slope and linear distance) and the third PC (9.7%) contains only data from the acoustic measurements of the sensory panel (panel number of sound peaks and panel maximum SPL).

4. CONCLUSIONS

The present work integrated the study of energy dissipative processes to the analysis of sound emission, crucial for understanding the crispy/crunchy nature of solid foods.

It is clear that in almonds sensory crispness is highly correlated with the rate of emission and size of acoustic peaks emitted by cracks, as previously observed in biscuits, and clearly detectable in the negative peaks of the second derivative of the force-displacement curve. This provides a consistent mechanistic explanation of crispness, which clearly differentiates materials with two separate objective measures; acoustic and mechanical. Macro- and micro-structural data supports our conclusions. The first PC contains both acoustic and mechanical measures. We conclude therefore that sensory crispness is evaluated both acoustically and mechanically and that both measures are necessary to most effectively describe crispness.

We have also shown that a chemometric approach in which complex acoustic and mechanical data are appropriately combined statistically provides an effective way of objectively measuring the sensory parameter 'crispness.' There is obvious potential for an economic and non-invasive objective measure of crispness with passive acoustics.

Acknowledgements

The authors are indebted to the Ministerio de Educación y Ciencia (Spain) for the grant awarded to author Paula Varela. We also would like to thank Stable Micro Systems for technical assistance. Malcolm Povey also wishes to thank Roy Goodaere of Manchester University for pointing out the utility of chemometrics in acoustic analysis.

REFERENCES

1. Vincent JFV. The quantification of crispness. *J. Sci. Food Agr.* 1998; **78**: 162–168.
2. Chen J, Karlsson C, Povey M. Acoustic Envelope Detector for crispness assessment of biscuits. *J. Texture Studies* 2005; **36**: 139–156.
3. Szczesniak A, Klein D. Consumer awareness of texture and other food attributes. *Food Technol.* 1963; **63**: 74–77.
4. Szczesniak A. The meaning of textural characteristics—crispness. *J. Texture Studies* 1988; **9**: 51–59.
5. Vickers Z, Bourne MC. A psycho-acoustic theory of crispness. *J. Food Sci.* 1976; **41**: 1158–1164.
6. Drake BK. Food crushing sounds. An introductory study. *J. Food Sci.* 1963; **28**: 233–241.
7. Sterling C, Simone MJ. Crispness in almonds. *Food Res.* 1954; **19**: 276–281.
8. Duizer L. A review of acoustic research for studying the sensory perception of crisp, crunchy and crackly textures. *Trends Food Sci. Technol.* 2001; **12**: 17–24.
9. Rodaut G, Dacremont C, Vallès Pamiès B, Colas B, Le Meste M. Crispness: a critical review on sensory and material science approaches. *Trends Food Sci. Technol.* 2002; **13**: 217–227.
10. Luyten A, Pluter JJ, Van Vliet T. Crispy/crunchy crusts of cellular solid foods: a literature review with discussion. *J. Texture Studies* 2004; **35**: 445–492.
11. Courcoux P, Chaunier L, DellaValle G, Lourdin D, Semenou M. Paired comparisons for the evaluation of crispness of cereal flakes by untrained assessors: correlation with descriptive analysis and acoustic measurements. *J. Chemom.* 2005; **19**: 129–137.
12. Tesch R, Normand M, Peleg M. Comparison of the acoustic and mechanical signatures of two cellular crunchy cereal foods at various water activity levels. *J. Sci. Food Agr.* 1996; **70**: 347–354.

DOI: 10.1002/cem

[13]. FAO, Faostat Statistics Database. Last updated February 2007. URL http://faostat.fao.org/site/567/desktopDefault.aspx?PageID=567
14. Pascual-Albero M, Pérez-Munuera I, Lluch MA. Cotyledon structure of raw, soaked and roasted almond (*Prunus amygdalus* L.). *Food Sci. Technol. Int.* 1998; **4**: 189–197.
15. Gou P, Guerrero L, Valero A, Arnau J, Romero A. Physico-chemical and sensory property changes in almonds of *Desmayo Largueta* variety during toasting. *Food Sci. Technol. Int.* 2000; **6**: 1–7.
16. *Association of Official Analytical Chemists, Official Methods of Analysis. 17th edition, AOAC, Gaithersburg, MD.* 2000.
17. Luyten H, Plijter J, Van Vliet T. Understanding the sensory attributes crispy and crunchy: an integrated approach. *In: Proceedings of the 3rd International Symposium on Food Rheology and Structure*, Fischer P, Marti I, Windhab EJ (Eds.). Zurich, ISBN 3-905609-19-3, 2003;.379–384.
18. Vincent JFV. The quantification of crispness. *J. Sci. Food Agr.* 1998; **78**: 162–168.
19. Van Vliet T, Luyten H. Fracture mechanics of solid foods. In *New physicochemical techniques for the characterization of complex food systems*, E Dickinson (ed.). Chapman & Hall: Cambridge, UK, 1995; 157–176.
20. Kinsler LE, Frey AR. *Fundamentals of acoustics*, 2nd edition. John Wiley & Sons, Inc.: New York, 1962; 108–127, 379–417.
21. Lillford P, van Vliet T, van de Velde F. Discussion session on solid foods. *Food Hydrocol.* 2006; **20**: 432–437.
22. Donald AM, Baker FS, Smith AC, Waldron KW. Fracture of plant tissues and walls as visualized by environmental scanning electron microscopy. *Annals Botany* 2003; **92**: 73–77.
23. Dang JMC, Copeland L. Studies of the fracture surface of rice grains using environmental scanning electron microscopy. *J. Sci. Food Agr.* 2004; **84**: 707–713.
24. Young CT, Schadel WE, Patee HE, Sanders TH. The microstructure of almond (Prunus dulcis (Mill.) D.A. Webb cv. 'Nonpareil') cotyledon. *LWT-Food Sci. Technol* 2004; **37**: 317–322.

DOI: 10.1002/cem